

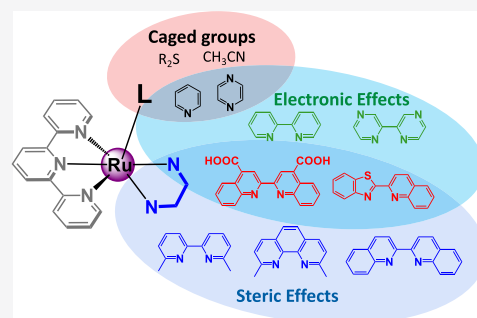
## Toward Optimal Ru(II) Photocages: Balancing Photochemistry, Stability, and Biocompatibility Through Fine Tuning of Steric, Electronic, and Physiochemical Features

Dmytro Havrylyuk, Kimberly Stevens, Sean Parkin, and Edith C. Glazer\*<sup>✉</sup>

Department of Chemistry, University of Kentucky, 505 Rose Street, Lexington, Kentucky 40506, United States

### Supporting Information

**ABSTRACT:** Ru(II) complex photocages are used in a variety of biological applications, but the thermal stability, photosubstitution quantum yield, and biological compatibility of the most commonly used Ru(II) systems remain unoptimized. Here, multiple compounds used in photocaging applications were analyzed and found to have several unsatisfactory characteristics. To address these deficiencies, three new scaffolds were designed to improve key properties through modulation of a combination of electronic, steric, and physiochemical features. One of these new systems, containing the 2,2'-biquinoline-4,4'-dicarboxylic acid (2,2'-bicinchoninic acid) ligand, fulfills several of the requirements for an optimal photocage. Another complex, containing the 2-benzothiazol-2-yl-quinoline ligand, provides a scaffold for the creation of “dual action” agents.



### INTRODUCTION

Photolabile systems are used in a variety of applications, ranging from materials to biomedical research.<sup>1,2</sup> Photons, coupled with compounds that can undergo photochemical transformation, provide the ability to control the location and timing for a physical effect through bond breakage or formation. Such systems are often termed “photocages”. Photocages are distinct from “photoswitches”<sup>3</sup> as the photochemical transformation is irreversible in a photocage. However, just like a photoswitch in the “off” position, it is essential that a photocage is biologically inert when intact. There must also be no activity from the empty “cage” to prevent interference with the biological effects from the released moiety (the caged ligand) under study.

While organic photocages have broad utility, metal centers were introduced as quasi-orthogonal protecting groups that could both expand the repertoire of the types of functional groups that can be “caged” and also shift absorption profiles into the visible and near-IR region. This allows for improved medical utility due to deeper penetration of photons, and it decreases the potential for adverse effects on cell health that is commonly induced by UV irradiation. Ru(II) complexes have been particularly effective for photocaging applications, and multiple groups have explored their use for photodelivery of drugs<sup>4–9</sup> and signaling molecules.<sup>10–19</sup>

In contrast to a standard photocage, metal-based systems can provide additional functions if the released metal is active itself. This results in “dual action” agents, where both the released ligand and the metal center each provide unique, preferably complementary biological effects.<sup>20,21</sup> While many of the desired features for optimal photocages and “dual action” agents are shared, the most important distinction is the

biological activity (or lack thereof) of the caging group following light irradiation. The released inorganic caging group is what we term the “scaffold”; it also serves as the synthetic building block for creating the photocaged complex when coordinated to biologically active ligands. The photochemistry and biological activity of the photocaged complex, and thus its utility, depends upon each of the associated spectator ligands, the three-dimensional structure of the complex, and the nature of the metal itself. We hypothesized that rationally varying the ligand components and structures of the metal complex could result in scaffolds with superior properties for photocaging applications. Alternatively, other scaffolds would function better as “dual action” agents.

In addition to the properties of the metal complex and associated ligands, the “caged” organic group plays an essential role. Different “caged” groups have been used by a variety of researchers, including imidazole, pyridine, diazines, amines, nitriles, and thioethers. Each of these functionalities can be incorporated in more sophisticated organic molecules for light-triggered release. For example, the seminal work in this area was performed by Etchenique, who developed phototriggered Ru(II) complexes that released nitrogen-containing neurotransmitters.<sup>10–16</sup> The Bonnet group demonstrated that thioethers such as *N*-acetylmethionine can be caged and released,<sup>22</sup> and Kodanko and Turro have shown a variety of nitriles can be similarly caged, such as peptide-based protease inhibitors.<sup>17,23</sup> Vasquez developed a Ru-coordinated histidine building block for Fmoc/*t*Bu solid-phase peptide synthesis, allowing for the development of caged peptides,<sup>24</sup> and Renfrew

Received: July 11, 2019

Published: January 3, 2020

has used imidazole-containing drugs for photodelivery.<sup>4–6</sup> Each of these and many other studies demonstrated different utilities of the basic system, but, to the best of our knowledge, there has not been a direct comparison of the most effective “caging” scaffolds or “caged” functional groups.

In previous work, we established that steric effects could be used to increase the quantum yields for photosubstitution ( $\Phi_{PS}$ ) of Ru(II) complexes used in biological applications.<sup>25–28</sup> Steric clash between the coordinated ligands results in elongation and/or distortion of metal–ligand bonds, and distortions within the ligand structure. These structural perturbations lower the energy of a dissociative <sup>3</sup>MC (metal centered) state, and allows for thermal population following photoexcitation to the <sup>3</sup>MLCT (metal to ligand charge transfer) state. Population of the <sup>3</sup>MC causes the ejection of a ligand.<sup>29–31</sup> This principle has been applied extensively to inorganic photocages by incorporating spectator ligands that induce steric clash.

Recently, we showed that electronic effects of the “caged” group could also be employed to regulate  $\Phi_{PS}$  in Ru(II) complexes,<sup>32</sup> providing an alternative strategy for fine-tuning of photochemistry. This project led us to investigate the interplay of steric and electronic features that impact the photochemistry of Ru(II) complexes. However, each structural modification impacted more than the single desired property, and thus altered the utility of a system for use as either a photocage or a “dual action” agent. A more systematic investigation was needed.

In this study we have focused on the impact of modulating steric and electronic features on five key properties: (1) the peak of the lowest energy absorption ( $\lambda_{max}$ ); (2) the photosubstitution quantum yield ( $\Phi_{PS}$ ); (3) stability under biological conditions (defined as % of intact compound remaining at a specific time point); (4) cytotoxicity in the dark; (5) cytotoxicity in the light. Cytotoxicity is normally quantified using  $EC_{50}$  or  $IC_{50}$  values, i.e., the effective or inhibitory concentration for 50% of the toxic effect. High values for items 1–4 are generally desirable for both a photocage and a “dual action” agent. In contrast, light-induced cytotoxicity (associated with a low  $IC_{50}$  value) is desired *only* in the case of a “dual action” agent; it would be detrimental in the case of a photocage.

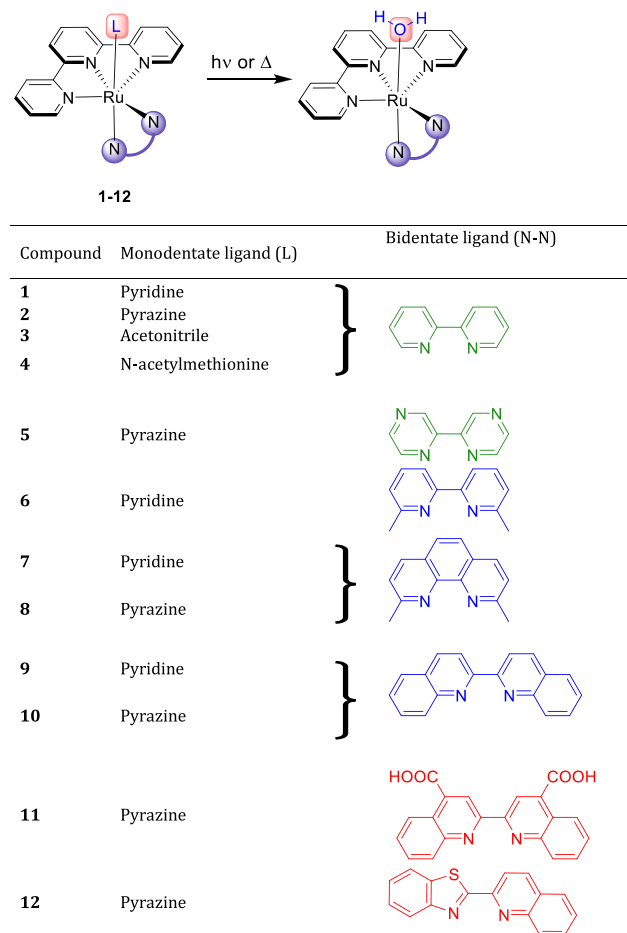
The majority of published Ru(II) compounds for photocaging applications possess considerable cytotoxicity of the intact form before irradiation, which limits the utility of these agents. Also, while there have been notable improvements of photophysical and photochemical features, reports of the thermal stability are inconsistent or have not been systematic; however, poor stability is a common problem for Ru(II) cages. In this work, we report our advances toward optimal Ru(II) photocages and “dual action” agents through the creation of new Ru(II) scaffolds. In pursuit of this goal, we also aimed to address the following key questions: (1) What is the impact of the most common “caged” organic functional groups on  $\Phi_{PS}$  and thermal stability? (2) What is the effect of bidentate spectator ligands that contribute steric bulk on key properties? (3) What features (electronic, steric, or both) would allow for the optimization of photocages or “dual action” agents? Finally, (4) how can biocompatibility be achieved?

## RESULTS

**Design and Synthesis.** Ru(II) complexes can potentially release multiple ligands, but for this study we focused on a

simple system that can only release one ligand. The complexes were designed as [Ru(tpy)(NN)L], where tpy = 2,2':6',2''-terpyridine, NN is a variety of bidentate ligands, and L is the “caged” monodentate ligand that can be released upon irradiation (Chart 1, top). The two chelating ligands were

Chart 1. Ru(II) Complexes Investigated in This Study<sup>a</sup>



<sup>a</sup>The scheme at the top depicts the photochemical or thermal ligand exchange of the monodentate ligand. The bidentate and monodentate ligands are varied in the complexes as shown. Ligand structures depicted in green reflect alterations in electronic properties, structures in blue reflect changes in the steric properties, and ligands shown in red exhibit a mixture of steric and electronic effects.

used as they are expected to remain bound to the metal. This ensures only a single photochemical product resulting from the loss of the monodentate ligand.

The tridentate tpy ligand was included in all complexes, and both the bidentate and monodentate ligands were then varied to investigate the effects of ligands that contributed steric bulk, electronic effects, or both. The monodentate ligands used were acetonitrile, N-acetylmethionine, pyridine, and pyrazine.<sup>33</sup> The bidentate systems studied were 2,2'-bipyridine (bpy), 2,2'-bipyrazine (bpz), 6,6'-dimethyl-2,2'-bipyridine (dmbpy), 2,9-dimethyl-1,10-phenanthroline (dmphe), 2,2'-biquinoline (biq), 2,2'-biquinoline-4,4'-dicarboxylic acid (2,2'-bicinchoinic acid, bca), and 2-benzothiazol-2-yl-quinoline (btz-qui). In total, 12 compounds were synthesized based on seven scaffolds to perform a detailed structure–property analysis.

First, we synthesized the most commonly used Ru(II) photocages according to published procedures (compounds 1,<sup>34</sup> 2,<sup>32</sup> 3,<sup>35</sup> 4,<sup>22</sup> 6,<sup>34</sup> and 9<sup>34</sup>), and evaluated their performance. The systems were then redesigned to improve key properties. Compounds 5, 7, 8, and 10–12 are novel compounds and were synthesized for the first time. The complexes were purified to ensure no contamination of either free ligands or coordinatively unsaturated Ru(II) centers. All the complexes are +2 charged except for complex 11, which is neutral, as the bca ligand contains two carboxylic acids that were deprotonated under the experimental conditions. The complexes were characterized by <sup>1</sup>H NMR spectroscopy, ESI-MS, X-ray, and UV/vis spectroscopy (see Figures S8–S18 and S23–S35 in the Supporting Information).

**Structure–Property Analysis of Photocaged Systems.** As shown in Figure 1, the absorption profiles of the different

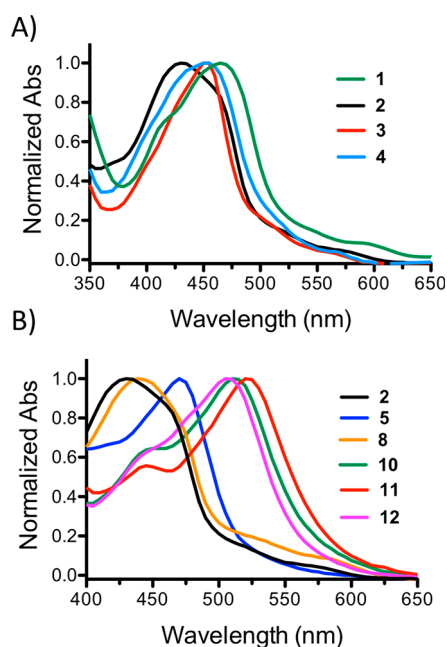


**Figure 1.** Comparison of normalized UV/vis profiles of Ru(II) complexes in H<sub>2</sub>O as a function of variation of the monodentate ligand (A) and bidentate ligand (B). Concentrations of ~10 μM were used in the measurements.

photocages varied slightly as a function of the monodentate “caged” ligand (Figure 1A) and more significantly with different bidentate ligands (Figure 1B). Both mono- and bidentate ligands had an impact on the  $\lambda_{\text{max}}$  and extinction coefficient ( $\epsilon$ ) values, with extended conjugation of the bidentate ligands inducing bathochromic shifts, as anticipated. In order to standardize photochemical evaluation, the  $\Phi_{\text{PS}}$  for all systems was determined using 470 nm light in H<sub>2</sub>O. Large variations were observed, with  $\Phi_{\text{PS}}$  ranging from <0.0001 to 0.141. The photophysical and photochemical characteristics are shown in Table 1.

A high thermal stability is needed for compounds to serve as useful photocages for most biological or materials applications. The stability of each complex was assessed over 24 and 72 h under aqueous conditions at 37 °C. First, the different photocaging functional groups, nitrile, thioether, pyridine, and pyrazine, were compared in complexes 1–4. Notably, the nitrile was the only monodentate ligand that created a thermally unstable complex (compound 3); compounds 1, 2,

and 4 exhibited no degradation over 24 h. However, they also exhibited 10-fold lower  $\Phi_{\text{PS}}$  than compound 3.

Next, the effect of strain-inducing spectator ligands on thermal stability was studied in complexes 6–10, and compared with  $\Phi_{\text{PS}}$ . Inclusion of dmbpy (6), dmphen (7), and biq (9) into [Ru(tpy)(NN)(py)] systems resulted in an inverse relationship between  $\Phi_{\text{PS}}$  and stability (Figure 3A). The compounds with the higher quantum yields (6 and 7, >0.05) degraded by 52–76% over 24 h (Table 1, Figure 2A). In contrast, there was a better retention of stability with an increase in  $\Phi_{\text{PS}}$  when electronic features were altered by changing the monodentate ligand from pyridine to pyrazine. However, the extent of this effect was found to be dependent on the identity of the strain-inducing ligand. For example, systems 7 vs 8 that contain the dmphen ligand exhibited a 7% increase in quantum yield upon substituting pyrazine for pyridine, but this was associated with a 40% reduction in the stability of the complex. The biq coligand was superior, as a 13% increase in quantum yield was associated with only a 20% reduction in stability with replacement of pyridine with pyrazine (complex 9, 10). However, none of the strain-inducing ligands produced thermally stable complexes on a 72 h time scale (Figure S22). This raised an obvious challenge: how to create a photocage with a sufficient  $\Phi_{\text{PS}}$  for utility without a concomitant loss in thermal stability.

**Strategies To Optimize the Photocaging Scaffold.** The suboptimal qualities of the commonly used cages motivated the investigation of alternative approaches to change the Ru(II) scaffold in order to increase  $\Phi_{\text{PS}}$  while maintaining stability. It is known that tris homoleptic Ru(II) complexes that contain the bipyrazine ligand are photolabile;<sup>36,37</sup> this is in contrast to the bipyridine ligand, which generally produces photostable complexes. Accordingly, the bipyrazine ligand was incorporated into a scaffold to form complex 5. Due to the *mer* arrangement of the tpy ligand, one of the bipyrazine rings is *trans* to the leaving ligand, so it was anticipated that the more electron deficient heterocycle would exert an effect through a shared orbital. However, while the switch from bpy to bpz resulted in a complex that was thermally stable, there was a loss in photochemical reactivity ( $\Phi_{\text{PS}} = 0.0007$  vs 0.0013 for the analogous complex 2 with bpy). This demonstrated that electronic modulations that work for the monodentate ligand<sup>32,38</sup> do not translate in this case for the bidentate ligand. Thus, the focus shifted to ligands that induce moderate steric clash compared to dmbpy and dmphen.

Following our demonstration of the use of 2,2'-biquinoline to make Ru(II) complexes that can be activated with red and near-IR light for biological applications,<sup>25</sup> this ligand has been successfully applied in the creation of several photocages.<sup>4,5,34,39–45</sup> However, complexes containing the biq ligand have notably higher cytotoxicity than complexes with bpy or phen ligands. This limits the utility of biq-containing systems as photocages in live cells. With the aim of reducing toxic effects while preserving the photoreactivity and low energy absorption, two strategies were investigated: adding negatively charged groups to biq to modulate physicochemical properties, and altering the core ligand structure.

To test the first approach, the 2,2'-biquinoline-4,4'-dicarboxylic acid (bca) ligand was incorporated, which resulted in the neutral Ru(II) complex 11. It was anticipated that the carboxylates would alter interactions with biomolecules responsible for the cytotoxicity in the absence of irradiation. In a second approach, the ligand structure of biq was modified

Table 1. Photophysical and Biological Properties

compound	$\lambda_{\text{abs}}^{\text{MLCT}}$ (nm) ( $\epsilon$ ( $\text{M}^{-1} \text{cm}^{-1}$ )) <sup>a</sup>	$\Phi_{\text{PS}}(\text{H}_2\text{O})$	stability <sup>b</sup>	$\text{IC}_{50}$ ( $\mu\text{M}$ ) <sup>c</sup>		$\text{PI}^{\text{d}}$
				dark	light	
1	468 (8,100) <sup>34</sup>	n.d.	100	>100	>100	—
2	430 (10,000) <sup>32</sup>	0.0013(2)	100	>100	>100	—
3	454 (10,900) <sup>35</sup>	0.0125(3)	84	>100	>100	—
4	452 (5,400) <sup>22</sup>	0.0027(2)	100	>100	>100	—
5	465 (6,100)	0.0007(2)	100	30 ± 2.8	24.2 ± 2.1	>1.2
6	471 (8,000) <sup>34</sup>	0.104(1)	34	>100	42.6 ± 2.5	>2.3
7	470 (12,000)	0.058(2)	48	>100	66 ± 9.6	>1.5
8	440 (10,000)	0.132(1)	8	>100	58.9 ± 6.3	>1.7
9	530 (9,000) <sup>34</sup>	0.014(2)	82	30.8 ± 1.9	11 ± 0.2	2.8
10	510 (9,900)	0.141(2)	63	34.6 ± 0.3	17.7 ± 0.1	1.9
11	520 (6,600)	0.121(2)	69	>100	>100	—
12	505 (8,300)	0.0368(4)	84	~100	27.6 ± 3.4	>3.6

<sup>a</sup>Indicates previously reported values. <sup>b</sup>Determined as % remaining at 24 h (37 °C) in H<sub>2</sub>O, calculated by optical and HPLC approaches. <sup>c</sup>Cytotoxicity of compounds evaluated in the HL-60 cell line (averages of three measurements). This cell line was chosen as it is sensitive to a variety of toxic agents, allowing for detection of biological effects that might not be observed in a more resistant cell line. The IC<sub>50</sub> value of cisplatin is 3.1 ± 0.3  $\mu\text{M}$  in this cell line. <sup>d</sup>The phototoxicity index (PI) is the ratio of the dark and light IC<sub>50</sub> values.

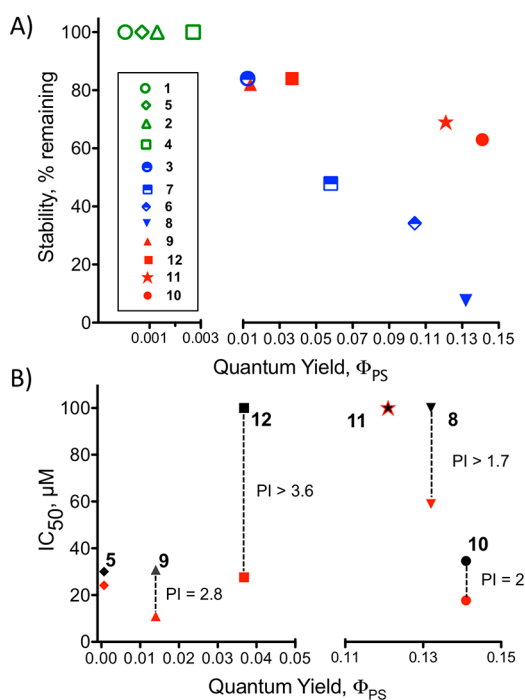


**Figure 2.** Key properties for photocages. (A) Correlation between  $\Phi_{\text{PS}}$  and stability (at 24 h). Green labels indicate compounds with high stability but low  $\Phi_{\text{PS}}$ ; red labels indicate compounds with  $\lambda_{\text{abs}} > 500$  nm; blue labels are used for compounds with strain-inducing ligands or a labile nitrile. (B) Correlation between  $\Phi_{\text{PS}}$  and cytotoxicity IC<sub>50</sub> (dark, black; light, red; the PI is shown for emphasis).

by replacement of one of the coordinating ring systems. This bidentate ligand, 2-benzothiazol-2-yl-quinoline (btz-qui), was used in complex 12. Complex 11 exhibited a slight increase in thermal stability (69 vs 63%) and a slight decrease in  $\Phi_{\text{PS}}$  compared to complex 10 (0.121 vs 0.141; Table 1). Complex 12 exhibited greater stability (84% remaining at 24 h) but a 3-fold lower  $\Phi_{\text{PS}}$  than the corresponding biq complex 10.

**Effect of Structure on  $\Phi_{\text{PS}}$  and Stability.** The structure of complex 12 was determined by X-ray crystallography in order to rationalize the modifications in stability and  $\Phi_{\text{PS}}$ . As

expected, the inclusion of the btz-qui ligand in complex 12 resulted in a distorted octahedral geometry. In contrast to Ru(II) complexes containing the analogous asymmetric pyridine–benzazole ligand,<sup>46</sup> where the two rings of the bidentate ligand are essentially coplanar, the benzothiazole–quinoline system of 12 exhibits a bowed shape (Figures 3A and S1). In addition, the btz-qui ligand is tilted from the N4–Ru–N5 plane, with a N5–Ru–N4–C22 torsion angle of 17.91° and a N4–Ru–N5–C23 torsion angle of 18.35° (Figure S1; selected bond lengths and angles are listed in Table S2). As the

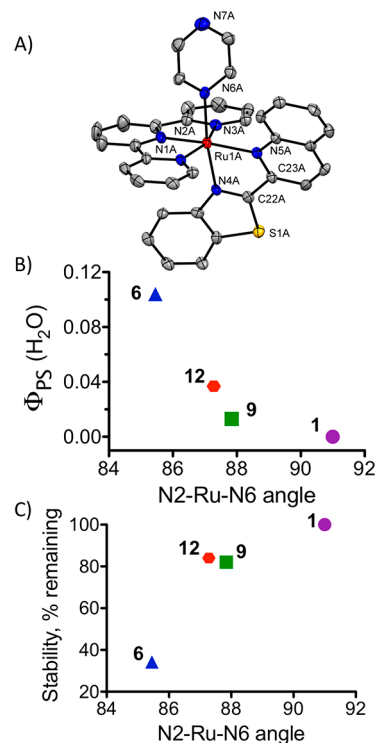


**Figure 3.** Effect of structure on  $\Phi_{\text{PS}}$  and stability. (A) Ellipsoid map of 12 with hydrogens omitted for clarity. (B) Correlation of  $\Phi_{\text{PS}}$  with selected bond angle demonstrates that there is an inverse relationship as the bond angle approaches 90°. (C) Stability increases as the selected bond angle approaches 90°.

bridging carbons are below the plane of the coordinating nitrogen, this results in slightly misdirected metal–ligand bonds.<sup>47</sup>

The Ru–N bond distances involving the tpy ligands are essentially unaltered with the btz-qui ligand in comparison to the biq ligand. However, the asymmetric btz-qui ligand resulted in a larger disparity of Ru–N4 and Ru–N5 bond distances (2.075 and 2.134 Å) compared to the corresponding complex **9** containing the symmetric biq coligand (Table S2, 2.101 and 2.115 Å).<sup>54</sup> The benzothiazole ring of the btz-qui ligand is coordinated *trans* to the labile pyrazine, and the Ru–N6 bond distance for the monodentate pyrazine ligand is also slightly shorter than distances to the pyridine in **1**, **6**, and **9** (from 0.012–0.026 Å). However, no correlation was observed between the bond length and  $\Phi_{PS}$  or stability of the complexes.

The bond angles between pyrazine ligand and tpy (N2–Ru–N6, 87.28°) or quinoline (N5–Ru–N6, 97.48°) are nonequivalent, indicating that pyrazine is significantly tilted toward the tpy ligand. Although the N2–Ru–N5 bond angles for the *trans* ligands are essentially identical in **9** and **12** (175.61° and 175.24°, respectively), the adjacent N5–Ru–N6 bond angle for **12** exhibits a larger distortion from the ideal 90° (at 97.5°). Importantly, the tilts of the monodentate ligands toward the N2 atom of the tpy ligand were found to correlate with both the stability of complexes and  $\Phi_{PS}$  in water for **1**, **6**, **9**, and **12**, as shown in Figure 3, parts B and C. This tilt results in a misdirected metal–ligand bond, which affects partitioning into the dissociative <sup>3</sup>MC (metal-centered state). Thus, the angle of the bond between the ligand and metal center appears more important than the bond lengths for photochemical and thermal features.

**Cytotoxicity Analysis.** A structure–activity analysis assessing cytotoxicity was performed aiming to identify the scaffolds with suitable biocompatibility. Cell death was determined after 72 h incubation with the complexes in the dark, or following a 1 h incubation and subsequent light exposure (22 J/cm<sup>2</sup>) before the 72 h incubation. Notably, in the dark, all photocages containing bpy, dmbpy, and dmphen ligands (**1–4**, **6–8**) were not cytotoxic at concentrations up to 100 μM. Surprisingly, the inclusion of the 2,2′-bipyrazine ligand resulted an IC<sub>50</sub> value of ca. 30 μM for **5**. Complexes **9** and **10**, which contain biq ligands, also were relatively toxic, and exhibited IC<sub>50</sub> values of ca. 30 μM. Thus, it was concluded that photocages containing biq and bpz ligands should be avoided due to their intrinsic cytotoxicity. Gratifyingly, complexes **11** and **12**, with the btz-qui and bca ligands, exhibited IC<sub>50</sub> values of 100 μM or higher in the dark.

Exposure to light increased the cytotoxicity of several complexes. To determine if toxicity was due to singlet oxygen (<sup>1</sup>O<sub>2</sub>) production, Singlet Oxygen Sensor Green, a fluorescent reporter, was used to determine the ability of the compounds **3–5** and **9–12** to create this toxic species. Tris(bipyridine)-ruthenium(II) ([Ru(bpy)<sub>3</sub>]<sup>2+</sup>) was used as a positive control, with a quantum yield for <sup>1</sup>O<sub>2</sub> production ( $\Delta_O$ ) of 0.22. In contrast to [Ru(bpy)<sub>3</sub>]<sup>2+</sup>, none of the compounds exhibited <sup>1</sup>O<sub>2</sub> production (Figure S7). An alternative explanation would be that the released ligands are toxic. There has been some controversy over tris-bidentate complexes that eject strained, bidentate ligands, where it is questioned if the ligand-deficient metal or the liberated ligand is the cytotoxic species.<sup>48–50</sup> However, the complexes that were most effective for cell killing ejected the monodentate pyridine and pyrazine, both of which are inactive.<sup>51</sup> This supports the interpretation that the specific

structure of the ligand-deficient Ru(II) complex is the component responsible for the observed activity, and this facilitates the construction of “dual action” agents.

In contrast to photocages, low IC<sub>50</sub> values would be desired for scaffolds used to create dual action agents. While complex **9** was the most potent (IC<sub>50</sub> = 11 μM), this complex has a small phototoxicity index (PI, Table 1, Figure 3B) due to the cytotoxicity of the complex in the dark. Complex **10** suffers from the same issue, but has a 10-fold higher  $\Phi_{PS}$  than **9**. While the IC<sub>50</sub> for complex **12** is more modest (27.6 μM), the lower toxicity in the dark (56% viable cells at 72 h post addition of 100 μM **12**) makes this the most promising scaffold. However, the specific mechanism by which the compound exerts a toxic effect remains to be established. Depending on the biological target of this complex, there may be the potential for synergy with a carefully chosen organic ligand.

## DISCUSSION

Ru(II) complexes have been used extensively for photocaging approaches. This includes applications in biology, as addressed in this report, but also in materials, for example for development of molecular machines,<sup>52</sup> surface modification,<sup>53</sup> or regulation of hydrogel properties.<sup>54</sup> However, to our knowledge there has not been a comparison of the properties of the most commonly used Ru(II) photocaging scaffolds or photoreleasable functional groups. As a result, scientists are utilizing systems that may not be optimal for the chosen application. Moreover, there are significant limitations to some of the most commonly applied Ru(II) photocage scaffolds. The most prominent drawbacks are lack of thermal stability and significant cytotoxicity.

Here, we considered five key properties: (1) absorption  $\lambda_{max}$ ; (2)  $\Phi_{PS}$ ; (3) stability under biological conditions; (4) cytotoxicity in the dark; and (5) cytotoxicity in the light. These parameters are depicted in the radar charts shown in Figure 4. In our view, an optimal “pure photocage” would exhibit long wavelength absorption, moderate  $\Phi_{PS}$  (to provide for facile activation by light but still allow for handling under experimental conditions), high thermal stability, and low cytotoxicity both before and after light activation. In contrast, an ideal “dual action” agent would have the same features, except for the fact that the scaffold would be cytotoxic following activation with light. It is the balance of these five features, rather than any one feature, that defines a good photocage or dual action scaffold.

Accordingly, the impact of both the photocaged functional group and the bidentate spectator ligand on each of these properties was assessed. The caged functional group was found to have a minor impact on  $\lambda_{max}$  (Figure 1A), but caused significant variation in  $\Phi_{PS}$  and stability (Figure 2A). Unfortunately, while nitriles have the higher  $\Phi_{PS}$ , this comes at the cost of some stability (16% degraded over 24 h). Either pyrazine or thioether functional groups were found to be preferable when thermal stability is an important feature, as these functional groups exhibited 100% stability over the same time period. Notably, none of the photocaged groups caused cytotoxicity in the dark or in the light. As the identity of the photocaging functional group (nitrile, thioether, pyridine, or pyrazine) can be changed if this is not essential for the activity of the liberated ligand, this information allows for the rational choice of the metal-binding component for improved photocages.

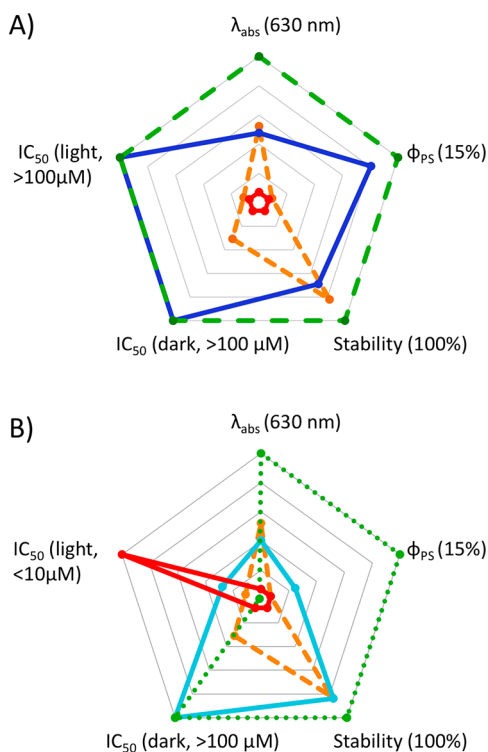


**Figure 4.** Radar charts for comparison of the key features for photocages (A) and dual action agents (B). (A) The “ideal pure photocage” (dashed green) compared with a hypothetical negative control (solid red), compound **9** (dashed orange), and **11** (solid blue). The axes scale from center to perimeter as follows: Absorbance, 420–630 nm;  $\Phi_{PS}$ , 0–15%; stability (%) and  $IC_{50}$  for cytotoxicity ( $\mu M$ ), 0–100. The desired parameters for an “ideal pure photocage” are indicated in parentheses. (B) The “ideal dual action agent” (dotted green) compared with the hypothetical negative control (solid red), compound **9** (dashed orange), and **12** (solid aqua). Note: the axes scales and desired parameters are the same as for part A except for the  $IC_{50}$  (light), which scales from 1–100  $\mu M$  from the center to perimeter. For a dual action agent, a low value is preferred.

The bidentate ligand had a larger impact on  $\lambda_{max}$ ; shifts of up to 100 nm were achieved by changing the chelating ligand (Figure 1B). There was also a 200-fold range in values for  $\Phi_{PS}$ , but enhanced photolability was associated with decreased thermal stability. The effect was structure dependent; notably poor thermal stabilities were found with complexes containing the dmbpy and dmphen ligands compared to biq or bca complexes with comparable  $\Phi_{PS}$  values (compounds **7**, **8**, **10**, and **11**; Figure 2A). Photocages containing biq, bca, and btz-qui ligands all exhibited longer wavelength  $\lambda_{max}$  values, and good  $\Phi_{PS}$ . The thermal stabilities were in the range of 63–84% at 24 h, making them potentially useful for shorter biological experiments. However, these findings demonstrate that complexes containing the biq ligand should be avoided in many experiments due to their intrinsic cytotoxicity, which does not require light activation. In contrast, compounds **7** and **8** exhibited low dark toxicities, but given their poor stability, these do not appear to be highly biocompatible scaffolds.

The redesign of the Ru(II) scaffold by incorporating carboxylic acids or changing one-half of the biq ligand resulted in complexes **11** and **12**. Both complexes exhibited low toxicity in the dark. In contrast to commonly used Ru(II) photocages, it appears that the scaffolds including the bca and btz-qui ligands are more biocompatible, and thus, suitable for

photobiological applications. Of course, the effect of each complex is anticipated to depend on several variables, including the specific cell line used, the compound exposure time, light dose, and time period of the experiments.<sup>55</sup> However, these results suggest that inclusion of negatively charged groups or other ligand modifications can be used to abrogate the cytotoxicity of Ru(II) complexes. This will be addressed in another report.

Notably, in complexes containing bidentate ligands *other* than bpy, photoejection was associated with an increase in cytotoxicity. However, PI values were generally modest. Of all the scaffolds that were nontoxic in the dark, the [Ru(tpy)(btz-qui)] scaffold in **12** provided the most significant increase in cytotoxicity (Figure 2B). These results encourage the use of this system in the development of “dual action” agents.

In contrast, the [Ru(tpy)(bca)] scaffold in **11** is preferred for pure photocaging applications. This system is nontoxic both in the dark and following activation by light. This lack of toxicity is desirable in cases where the activity of the liberated ligand is the focus, and effects of other active species in the biological environment will only confuse the results. Moreover, the complex has a high  $\Phi_{PS}$  in water, and sufficient stability to allow for experiments that require hours of exposure time. We propose that the use of this scaffold will improve the performance of Ru(II) based photocages.

## CONCLUSION

This work demonstrates the steric, electronic, and physicochemical features that can be used to tune photochemistry of Ru(II) complexes. While the results are most directly relevant for work that utilizes these coordination complexes for biological applications, the findings are also applicable for any systems that rely on Ru(II) photochemical transformations. Scientists can use the data described here to choose the optimal scaffold for their specific application needs based on the various characteristics of  $\lambda_{max}$ ,  $\Phi_{PS}$ , stability, and biological compatibility both before and after light-mediated release of coordinated ligands.

## ASSOCIATED CONTENT

### Supporting Information

The Supporting Information is available free of charge at <https://pubs.acs.org/doi/10.1021/acs.inorgchem.9b02065>.

General information on synthetic methods, characterization, photochemical and photobiological analysis, and additional figures (PDF)

### Accession Codes

CCDC 1901015 contains the supplementary crystallographic data for this paper. These data can be obtained free of charge via [www.ccdc.cam.ac.uk/data\\_request/cif](http://www.ccdc.cam.ac.uk/data_request/cif), or by emailing [data\\_request@ccdc.cam.ac.uk](mailto:data_request@ccdc.cam.ac.uk), or by contacting The Cambridge Crystallographic Data Centre, 12 Union Road, Cambridge CB2 1EZ, UK; fax: +44 1223 336033.

## AUTHOR INFORMATION

### Corresponding Author

\*(E.C.G.) E-mail: [ec.glazer@uky.edu](mailto:ec.glazer@uky.edu).

### ORCID

Edith C. Glazer: 0000-0002-0190-7742

### Author Contributions

The manuscript was written through contributions of all authors. All authors have given approval to the final version of the manuscript.

### Notes

The authors declare no competing financial interest.

### ACKNOWLEDGMENTS

We gratefully acknowledge the National Institutes of Health (Grant GM107586) for the support of this research. Crystallographic work was made possible by the National Science Foundation (NSF) MRI program, grants CHE-0319176 and CHE-1625732.

### REFERENCES

- (1) Ankenbruck, N.; Courtney, T.; Naro, Y.; Deiters, A. Optochemical Control of Biological Processes in Cells and Animals. *Angew. Chem., Int. Ed.* **2018**, *57* (11), 2768–2798.
- (2) Russev, M. M.; Hecht, S. Photoswitches: from Molecules to Materials. *Adv. Mater.* **2010**, *22* (31), 3348–3360.
- (3) Velema, W. A.; Szymanski, W.; Feringa, B. L. Photopharmacology: Beyond Proof of Principle. *J. Am. Chem. Soc.* **2014**, *136* (6), 2178–2191.
- (4) Wei, J.; Renfrew, A. K. Photolabile Ruthenium Complexes to Cage and Release a Highly Cytotoxic Anticancer Agent. *J. Inorg. Biochem.* **2018**, *179*, 146–153.
- (5) Chan, H.; Ghayche, J. B.; Wei, J.; Renfrew, A. K. Photolabile Ruthenium(II)-Purine Complexes: Phototoxicity, DNA Binding, and Light-Triggered Drug Release. *Eur. J. Inorg. Chem.* **2017**, *2017* (12), 1679–1686.
- (6) Karaoun, N.; Renfrew, A. K. A Luminescent Ruthenium(II) Complex for Light-Triggered Drug Release and Live Cell Imaging. *Chem. Commun.* **2015**, *51* (74), 14038–14041.
- (7) Smith, N. A.; Zhang, P.; Greenough, S. E.; Horbury, M. D.; Clarkson, G. J.; McFeely, D.; Habtemariam, A.; Salassa, L.; Stavros, V. G.; Dowson, C. G.; Sadler, P. J. Combatting AMR: Photoactivatable Ruthenium(II)-isoniazid Complex Exhibits Rapid Selective Antimicrobial Activity. *Chem. Sci.* **2017**, *8* (1), 395–404.
- (8) Li, A.; Yadav, R.; White, J. K.; Herroon, M. K.; Callahan, B. P.; Podgorski, I.; Turro, C.; Scott, E. E.; Kodanko, J. J. Illuminating Cytochrome P450 Binding: Ru(II)-Caged Inhibitors of CYP17A1. *Chem. Commun.* **2017**, *53* (26), 3673–3676.
- (9) Zamora, A.; Denning, C. A.; Heidary, D. K.; Wachter, E.; Nease, L. A.; Ruiz, J.; Glazer, E. C. Ruthenium-containing P450 Inhibitors for Dual Enzyme Inhibition and DNA Damage. *Dalton Trans.* **2017**, *46*, 2165–2173.
- (10) Zayat, L.; Calero, C.; Albores, P.; Baraldo, L.; Etchenique, R. A New Strategy for Neurochemical Photodelivery: Metal-Ligand Heterolytic Cleavage. *J. Am. Chem. Soc.* **2003**, *125* (4), 882–883.
- (11) Nikolenko, V.; Yuste, R.; Zayat, L.; Baraldo, L. M.; Etchenique, R. Two-Photon Uncaging of Neurochemicals Using Inorganic Metal Complexes. *Chem. Commun.* **2005**, No. 13, 1752–1754.
- (12) Zayat, L.; Salierno, M.; Etchenique, R. Ruthenium(II) Bipyridyl Complexes as Photolabile Caging Groups for Amines. *Inorg. Chem.* **2006**, *45* (4), 1728–1731.
- (13) Zayat, L.; Filevich, O.; Baraldo, L. M.; Etchenique, R. Ruthenium Polypyridyl Phototriggers: from Beginnings to Perspectives. *Philos. Trans. R. Soc., A* **2013**, *371*, 20120330.
- (14) San Miguel, V.; Alvarez, M.; Filevich, O.; Etchenique, R.; del Campo, A. Multiphoton Reactive Surfaces Using Ruthenium(II) Photocleavable Cages. *Langmuir* **2012**, *28* (2), 1217–1221.
- (15) Salierno, M.; Marceca, E.; Peterka, D. S.; Yuste, R.; Etchenique, R. A Fast Ruthenium Polypyridine Cage Complex Photoreleases Glutamate with Visible or IR Light in One and Two Photon Regimes. *J. Inorg. Biochem.* **2010**, *104* (4), 418–422.
- (16) Fino, E.; Araya, R.; Peterka, D. S.; Salierno, M.; Etchenique, R.; Yuste, R. RuBi-Glutamate: Two-Photon and Visible-Light Photo-activation of Neurons and Dendritic Spines. *Front. Neural Circuits* **2009**, *3*, 2.
- (17) Li, A.; Turro, C.; Kodanko, J. J. Ru(II) Polypyridyl Complexes as Photocages for Bioactive Compounds Containing Nitriles and Aromatic Heterocycles. *Chem. Commun.* **2018**, *54* (11), 1280–1290.
- (18) Cabrera, R.; Filevich, O.; Garcia-Acosta, B.; Athilingam, J.; Bender, K. J.; Poskanzer, K. E.; Etchenique, R. A Visible-Light-Sensitive Caged Serotonin. *ACS Chem. Neurosci.* **2017**, *8* (5), 1036–1042.
- (19) Pereira, A. d. C.; Ford, P. C.; da Silva, R. S.; Bendhack, L. M. Ruthenium-Nitrite Complex as Pro-Drug Releases NO in a Tissue and Enzyme-Dependent Way. *Nitric Oxide* **2011**, *24* (4), 192–198.
- (20) Petruzzella, E.; Braude, J. P.; Aldrich-Wright, J. R.; Gandin, V.; Gibson, D. A Quadruple-Action Platinum(IV) Prodrug with Anticancer Activity Against KRAS Mutated Cancer Cell Lines. *Angew. Chem., Int. Ed.* **2017**, *56*, 11539–11544.
- (21) Bonnet, S. Why Develop Photoactivated Chemotherapy? *Dalton Trans.* **2018**, *47* (31), 10330–10343.
- (22) Goldbach, R. E.; Rodriguez-Garcia, I.; van Lenthe, J. H.; Siegler, M. A.; Bonnet, S. N-acetylmethionine and Biotin as Photocleavable Protective Groups for Ruthenium Polypyridyl Complexes. *Chem. - Eur. J.* **2011**, *17* (36), 9924–9929.
- (23) Respondek, T.; Garner, R. N.; Herroon, M. K.; Podgorski, I.; Turro, C.; Kodanko, J. J. Light Activation of a Cysteine Protease Inhibitor: Caging of a Peptidomimetic Nitrile with Ru(II)(bpy)<sub>2</sub>. *J. Am. Chem. Soc.* **2011**, *133* (43), 17164–17167.
- (24) Mosquera, J.; Sanchez, M. I.; Mascarenas, J. L.; Eugenio Vazquez, M. Synthetic Peptides Caged on Histidine Residues with a Bisbipyridyl Ruthenium(II) Complex that can be Photolyzed by Visible Light. *Chem. Commun.* **2015**, *51* (25), 5501–5504.
- (25) Wachter, E.; Heidary, D. K.; Howerton, B. S.; Parkin, S.; Glazer, E. C. Light-Activated Ruthenium Complexes Photobind DNA and are Cytotoxic in the Photodynamic Therapy Window. *Chem. Commun.* **2012**, *48* (77), 9649–9651.
- (26) Howerton, B. S.; Heidary, D. K.; Glazer, E. C. Strained Ruthenium Complexes Are Potent Light-Activated Anticancer Agents. *J. Am. Chem. Soc.* **2012**, *134* (20), 8324–8327.
- (27) Wachter, E.; Howerton, B. S.; Hall, E. C.; Parkin, S.; Glazer, E. C. A New Type of DNA “Light Switch”: a Dual Photochemical Sensor and Metalating Agent for Duplex and G-Quadruplex DNA. *Chem. Commun.* **2014**, *50* (3), 311–313.
- (28) Hidayatullah, A. N.; Wachter, E.; Heidary, D. K.; Parkin, S.; Glazer, E. C. Photoactive Ru(II) Complexes with Dioxinophenanthroline Ligands are Potent Cytotoxic Agents. *Inorg. Chem.* **2014**, *53* (19), 10030–10032.
- (29) Van Houten, J.; Watts, R. J. Temperature Dependence of the Photophysical and Photochemical Properties of the Tris(2,2'-bipyridyl)ruthenium(II) Ion in Aqueous Solution. *J. Am. Chem. Soc.* **1976**, *98* (16), 4853–4858.
- (30) Durham, B.; Caspar, J. V.; Nagle, J. K.; Meyer, T. J. Photochemistry of Ru(bpy)<sub>3</sub><sup>2+</sup>. *J. Am. Chem. Soc.* **1982**, *104* (18), 4803–4810.
- (31) Ford, P. C. The Ligand-Field Photosubstitution Reactions of D6 Hexacoordinate Metal-Complexes. *Coord. Chem. Rev.* **1982**, *44* (1), 61–82.
- (32) Havrylyuk, D.; Deshpande, M.; Parkin, S.; Glazer, E. C. Ru(II) complexes with Diazine Ligands: Electronic Modulation of the Coordinating Group Is Key to the Design of “Dual Action” Photoactivated Agents. *Chem. Commun.* **2018**, *54* (88), 12487–12490.
- (33) While imidazole systems can be easily synthesized, we found the photoreactivity to be too low for many applications.
- (34) Knoll, J. D.; Albani, B. A.; Durr, C. B.; Turro, C. Unusually Efficient Pyridine Photodissociation from Ru(II) Complexes with Sterically Bulky Bidentate Ancillary Ligands. *J. Phys. Chem. A* **2014**, *118* (45), 10603–10610.
- (35) Hecker, C. R.; Fanwick, P. E.; McMillin, D. R. Evidence for Dissociative Photosubstitution Reactions of [Ru(trpy)(bpy)-

(NCCH<sub>3</sub>)<sub>2</sub>)<sup>2+</sup>. Crystal and Molecular Structure of [Ru(trpy)(bpy)(py)](PF<sub>6</sub>)<sub>2</sub>·(CH<sub>3</sub>)<sub>2</sub>CO. *Inorg. Chem.* **1991**, *30* (4), 659–666.

(36) Crutchley, R. J.; Lever, A. B. P. Comparative Chemistry of Bipyrazyl and Bipyridyl Metal Complexes: Spectroscopy, Electrochemistry, and Photoanation. *Inorg. Chem.* **1982**, *21* (6), 2276–2282.

(37) Vicendo, P.; Mouysset, S.; Paillous, N. Comparative Study of Ru(bpz)<sub>3</sub>(2+) Ru(bipy)<sub>3</sub>(2+) and Ru(bpz)<sub>2</sub>Cl<sub>2</sub> as Photosensitizers of DNA Cleavage and Adduct Formation. *Photochem. Photobiol.* **1997**, *65* (4), 647–655.

(38) Vu, A. T.; Santos, D. A.; Hale, J. G.; Garner, R. N. Tuning the Excited State Properties of Ruthenium(II) Complexes with a 4-substituted Pyridine Ligand. *Inorg. Chim. Acta* **2016**, *450*, 23–29.

(39) Sun, W.; Wen, Y.; Thiramanas, R.; Chen, M.; Han, J.; Gong, N.; Wagner, M.; Jiang, S.; Meijer, M. S.; Bonnet, S.; Butt, H.-J.; Mailänder, V.; Liang, X.-J.; Wu, S. Red-Light-Controlled Release of Drug-Ru Complex Conjugates from Metallopolymer Micelles for Phototherapy in Hypoxic Tumor Environments. *Adv. Funct. Mater.* **2018**, *28*, 1804227.

(40) Sun, W.; Thiramanas, R.; Slep, L. D.; Zeng, X.; Mailänder, V.; Wu, S. Photoactivation of Anticancer Ru Complexes in Deep Tissue: How Deep Can We Go? *Chem. - Eur. J.* **2017**, *23*, 10832–10837.

(41) Chen, Z.; Sun, W.; Butt, H. J.; Wu, S. Upconverting-Nanoparticle-Assisted Photochemistry Induced by Low-Intensity Near-Infrared Light: How Low Can We Go? *Chem. - Eur. J.* **2015**, *21*, 9165–9170.

(42) Albani, B. A.; Durr, C. B.; Turro, C. Selective Photoinduced Ligand Exchange in a New Tris-Heteroleptic Ru(II) Complex. *J. Phys. Chem. A* **2013**, *117*, 13885–13892.

(43) Loftus, L. M.; White, J. K.; Albani, B. A.; Kohler, L.; Kodanko, J. J.; Thummel, R. P.; Dunbar, K. R.; Turro, C. New RuII Complex for Dual Activity: Photoinduced Ligand Release and IO<sub>2</sub> Production. *Chem. - Eur. J.* **2016**, *22*, 3704–3708.

(44) Woods, J. J.; Cao, J.; Lippert, A. R.; Wilson, J. J. Characterization and Biological Activity of a Hydrogen Sulfide-Releasing Red Light-Activated Ruthenium(II) Complex. *J. Am. Chem. Soc.* **2018**, *140*, 12383–12387.

(45) Lameijer, L. N.; Ernst, D.; Hopkins, S. L.; Meijer, M. S.; Askes, S. H. C.; Le Devedec, S. E.; Bonnet, S. A Red-Light-Activated Ruthenium-Caged NAMPT Inhibitor Remains Phototoxic in Hypoxic Cancer Cells. *Angew. Chem., Int. Ed.* **2017**, *56*, 11549–11553.

(46) Havrylyuk, D.; Heidary, D. K.; Nease, L.; Parkin, S.; Glazer, E. C. Photochemical Properties and Structure-Activity Relationships of RuII Complexes with Pyridylbenzazole Ligands as Promising Anticancer Agents. *Eur. J. Inorg. Chem.* **2017**, *2017* (12), 1687–1694.

(47) Ashby, M. T. Inverse Relationship Between the Kinetic and Thermodynamic Stabilities of the Misdirected Ligand Complexes Delta/Lambda-(Delta/Lambda-1,1'-Biisoquinoline)Bis(2,2'-Bipyridine)Metal(II) (Metal = Ruthenium, Osmium). *J. Am. Chem. Soc.* **1995**, *117*, 2000–2007.

(48) Cuello-Garibo, J. A.; Meijer, M. S.; Bonnet, S. To Cage or to Be Caged? The Cytotoxic Species in Ruthenium-Based Photoactivated Chemotherapy is Not Always the Metal. *Chem. Commun.* **2017**, *53*, 6768–6771.

(49) Azar, D. F.; Audi, H.; Farhat, S.; El-Sibai, M.; Abi-Habib, R. J.; Khnayzer, R. S. Phototoxicity of Strained Ru(II) Complexes: Is it the Metal Complex or the Dissociating Ligand? *Dalton Trans.* **2017**, *46*, 11529–11532.

(50) Mansour, N.; Mehanna, S.; Mroueh, M. A.; Audi, H.; Bodman-Smith, K.; Daher, C. F.; Taleb, R. I.; El-Sibai, M.; Khnayzer, R. S. Photoactivatable Ru(II) Complex Bearing 2,9-Diphenyl-1,10-phenanthroline: Unusual Photochemistry and Significant Potency on Cisplatin-Resistant Cell Lines. *Eur. J. Inorg. Chem.* **2018**, *2018*, 2524–2532.

(51) While recent reports have highlighted the cytotoxicity of some of the bidentate ligands used here, our HPLC analysis does not show any ejection of the bidentate ligand.

(52) Mobian, P.; Kern, J. M.; Sauvage, J. P. Light-Driven Machine Prototypes Based on Dissociative Excited States: Photoinduced Decoordination and Thermal Recoordination of a Ring in a

Ruthenium(II)-Containing [2]catenane. *Angew. Chem., Int. Ed.* **2004**, *43*, 2392–2395.

(53) Xie, C.; Sun, W.; Lu, H.; Kretzschmann, A.; Liu, J.; Wagner, M.; Butt, H. J.; Deng, X.; Wu, S. Reconfiguring Surface Functions Using Visible-Light-Controlled Metal-Ligand Coordination. *Nat. Commun.* **2018**, *9*, 3842.

(54) Rapp, T. L.; Wang, Y.; Delessio, M. A.; Gau, M. R.; Dmochowski, I. J. Designing photolabile ruthenium polypyridyl crosslinkers for hydrogel formation and multiplexed, visible-light degradation. *RSC Adv.* **2019**, *9* (9), 4942–4947.

(55) Monro, S.; Colon, K. L.; Yin, H.; Roque, J., 3rd; Konda, P.; Gujar, S.; Thummel, R. P.; Lilge, L.; Cameron, C. G.; McFarland, S. A. Transition Metal Complexes and Photodynamic Therapy from a Tumor-Centered Approach: Challenges, Opportunities, and Highlights from the Development of TLD1433. *Chem. Rev.* **2019**, *119* (2), 797–828.